Adsorption Equilibrium of the Mixture $CH_4 + N_2 + H_2$ on Activated Carbon

Qin Wu,[†] Li Zhou,*[,†] Jiaquan Wu,[†] and Yaping Zhou[‡]

High Pressure Adsorption Laboratory (State Key Laboratory of Chemical Engineering), School of Chemical Engineering and Technology, and Department of Chemistry, School of Science, Tianjin University, Tianjin 300072, China

Adsorption equilibrium data of the mixture $CH_4 + N_2 + H_2$ on activated carbon JX101 were collected with a dynamic method for the temperature range 283 K to 313 K. Since the critical temperature of the components is much lower than the temperature tested, this set of data was used to test the applicability of the available prediction models for the condition of above-critical temperatures. Some models rely on the adsorption data of pure components; therefore, the adsorption isotherms of pure CH_4, N_2, and H_2 on the same carbon were also collected. Six prediction models were tested. They are the extended Langmuir (EL) model, the loading ratio correlation (LRC) model, the ideal adsorption solution theory (IAST), the Flory−Huggins vacancy solution model (FHVSM), the model based on micropore size distribution and the extended Langmuir equation (MPSD−EL), and the model based on micropore size distribution and the ideal adsorption solution theory (MPSD−IAST). The performance of a model was valued with the average relative discrepancy between the experimental data and the model-predicted values.

Introduction

Multicomponent adsorption data are necessary information for designing a separation process based on adsorption.[1] Experimental collection of the adsorption equilibrium data of a mixture is a very tedious and time-consuming process. Therefore, it is preferable to estimate the multicomponent adsorption equilibrium on the basis of the adsorption isotherms of pure components. While a number of models have been developed for this purpose, prediction of the multicomponent adsorption remains a challenge. It becomes even more difficult if the mixture is at the supercritical condition. The prediction of multicomponent adsorption equilibrium will significantly affect the prediction of multicomponent sorption kinetics. Any error in the former would cause a large error in the latter.[2] Adsorption is an efficient tool in dealing with separation problems of gas mixtures composed of small molecules. Because the critical temperature of such gases is low, the mixture is usually supercritical at the temperature of engineering interest. Therefore, appropriate selection of the model is important. The applicability of the models available in the literature was tested with the experimental data of the supercritical mixture presently. The models tested include the following: (1) the extended Langmuir (EL) model, (2) the loading ratio correlation (LRC) model,[3−5] (3) the ideal adsorption solution theory (IAST) of Myers and Prausnitz,[6] (4) the Flory−Huggins vacancy solution model (FHVSM),[7−9] (5) the model based on micropore size distribution and the extended Langmuir equation (MPSD−EL),[10−13] and (6) the model based on micropore size distribution and the ideal adsorption solution theory (MPSD−IAST).[14,15]

* To whom correspondence should be addressed. Phone and fax: +86 22 87891466. E-mail: zhouli-tju@eyou.com.
[†] School of Chemical Engineering and Technology.
[‡] School of Science.

Experimental Section

Apparatus and Materials. Activated carbon JX101 (Tangshan Activated Carbon Company, China) with a particle size of 0.35 mm to 0.45 mm and a bulk density of 0.45 g/mL was used for the adsorbent. The sample was characterized on the basis of the adsorption isotherm of CO_2 at 273 K, which was collected on a volumetric setup. The details of the apparatus were previously described.[16,17] This apparatus has been used for many other studies, and it was used for collecting the adsorption isotherms of pure components presently. The carbon sample has a surface area of 1500 m^2/g. The micropore volume is 0.5 mL/g, and the total pore volume is 0.52 mL/g. High purity methane (≥99.99%), nitrogen (≥99.999%), and hydrogen (≥99.999%) were used as the adsorptives. The experimental conditions covered a temperature range of 283 K to 313 K. The pressure range was 0 to 1 MPa for the measurements of pure component adsorption and 0 to 0.6 MPa for the measurements of mixture adsorption.

The basic methods of collecting multicomponent adsorption data applied in the literature are the following: (1) the volumetric method,[18] (2) the gravimetric method,[19] (3) the open flow method including the differential adsorption bed (DAB) method,[13,20] and (4) the dynamic adsorption method.[21] Each method has some advantages and disadvantages. The dynamic method was selected in the present work. This method is just to collect breakthrough curves. It needs less time to reach equilibrium for supercritical gases and is especially convenient for the experimental condition of invariable pressure or invariable concentration. The measurement result can be directly presented in a figure.

All constraints for the dynamic method[4] to correctly yield the equilibrium data were carefully considered and satisfied.[22] The experimental apparatus is schematically shown in Chart 1. The adsorber is a stainless steel tube of a 250 mm length and 12 mm i.d. It was immersed in the water

10.1021/je049643a CCC: $30.25
Published on Web 01/25/2005

Chart 1. Schematic Diagram of the Dynamic Adsorption Measurement Apparatus

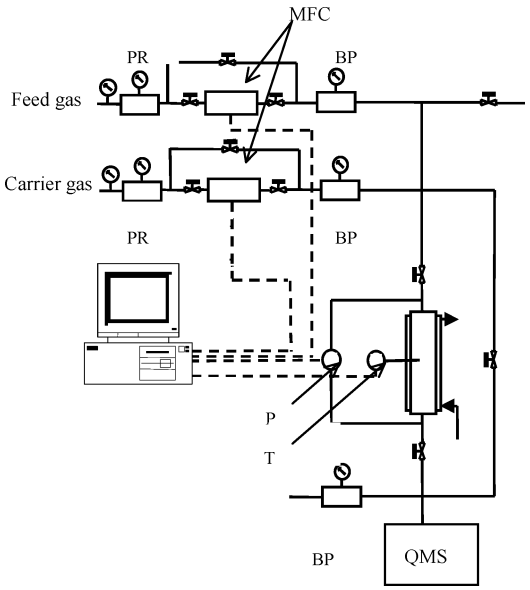

PR, pressure regulator; MFC, mass flow controller; BP, back-pressure regulator; P, pressure transducer; T, T-type thermocouple; QMS, gas analyzer.

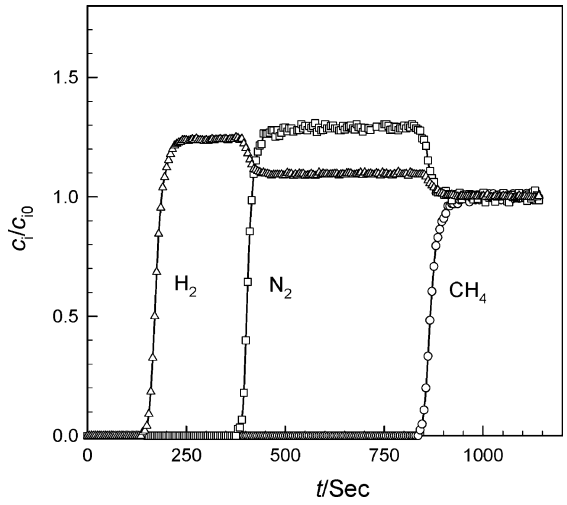

Figure 1. Breakthrough curves of the mixture through the adsorption bed.

bath of a thermostat. Two mass flow controllers were used to control the flow rates of the stream entering the adsorber: one for the ternary gas mixture and the other for the carrier gas (helium). A back-pressure regulator was used to maintain the pressure at the desired level. The system pressure was measured with a pressure transducer (PAA-23/8465.1-80). The deviation of pressure readings from linearity is ±0.1% for the full scale of 8 MPa. Three T-type thermocouples were used to measure the temperature at the entrance, midpoint, and exit of the adsorption bed. The composition of the exit stream was online analyzed by a residual gas analyzer (RGA100, Stanford Research Systems). The apparatus was connected to a computer. All experiments were automatically conducted according to a prescribed program.

Determination of the Equilibrium Amount Adsorbed for Each Component. The dynamic method yields breakthrough curves such as those shown in Figure 1, where c_0 and c are the initial concentration and the concentration at time t, respectively. The amount adsorbed

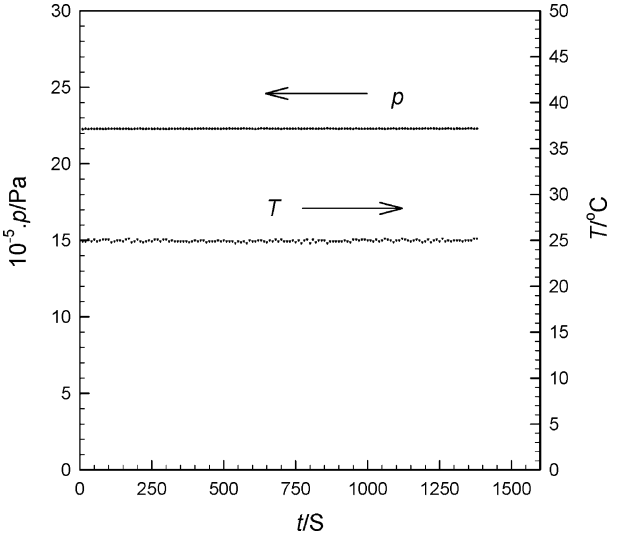

Figure 2. Recorded temperature and pressure at the center of the adsorption bed.

of a component can be evaluated from the breakthrough curves of the mixture.[23,24] For a given adsorption bed, we have the mass balance of component k:

$$\int_0^t u_i A c y_{k,i}\,\mathrm{d}t = \int_0^t u_e A c y_{k,e}\,\mathrm{d}t + \epsilon A L y_{k,i} p/RT + m n_k \quad (1)$$

where u_i and u_e are the linear flow speed at the entrance and exit of the adsorption bed, respectively; A and L are the section area and length of the adsorption bed; c is the total concentration of the gas stream; $y_{k,i}$ and $y_{k,e}$ are the concentration of component k in the gas stream at the entrance and exit of the adsorption bed, respectively; ϵ is the fractional void of the adsorption bed and can be evaluated in the volumetric setup of the adsorption measurement; and m is the mass of the adsorbent. The amount adsorbed of component k is then

$$n_k = \frac{\int_0^t (u_i y_{k,i} - u_e y_{k,e}) A c\,\mathrm{d}t - \epsilon A L y_{k,i} p/RT}{m} \quad (2)$$

The stream composition at the bed entrance is maintained constant, but that at the exit is a function of time for a definite period and the breakthrough curve is thus formed. The integration was evaluated numerically with the compound Simpson formula.

Discussion on the Reliability of the Dynamic Method. There are rigorous constraints for the dynamic method to guarantee the equilibrium data are reliable.[4] The invariable temperature, invariable pressure, dilute concentration of the gas mixture, and plug flow are the major conditions with which the experiments must comply. As shown in Figure 2, the temperature and pressure of the adsorption bed are almost constant. All the other concerns have also been carefully taken into account in our experiments.[22] As a test of the reliability of the dynamic method, a comparison between the adsorption isotherms of a pure gas determined by both static and dynamic measurement methods was made. It is well accepted that the volumetric method is perhaps one of the most reliable ways to collect the adsorption equilibrium data, and the dynamic method yielded almost the same isotherm, as shown in Figure 3.

Experimental Conditions and the Results. The adsorption equilibrium data of pure CH_4, N_2, and H_2 on activated carbon JX101 are listed in Tables 1−3 for temperatures of (283, 298, and 313) K and pressures up to

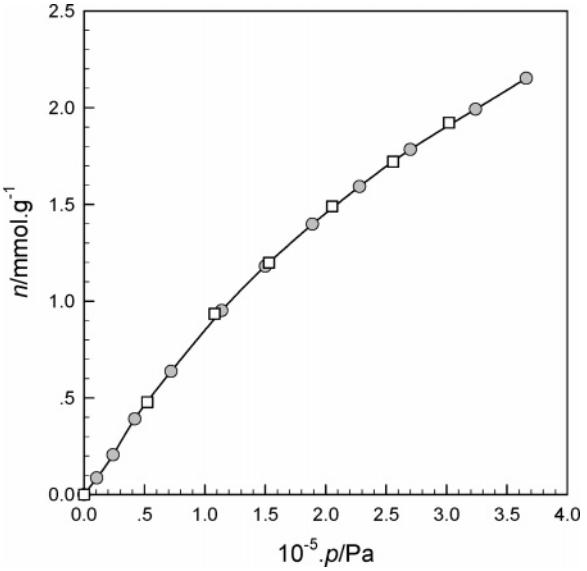

Figure 3. Comparison of the adsorption isotherms of CH_4 on activated carbon obtained by static and dynamic adsorption measurements: ●, by the volumetric method; □, by the dynamic method.

Table 1. Adsorption Data of CH_4 on Activated Carbon JX101

T/K					
283		298		313	
$10^{-5}p$/Pa	n/mmol·g^{-1}	$10^{-5}p$/Pa	n/mmol·g^{-1}	$10^{-5}p$/Pa	n/mmol·g^{-1}
.1650	.2543	.1050	.0853	.1800	.1217
.4350	.6328	.2400	.2051	.3900	.2623
.8400	1.0393	.4200	.3911	.6450	.4381
1.3500	1.4713	.7200	.6367	.9750	.6367
1.9800	1.8793	1.1400	.9511	1.3800	.8400
2.6550	2.2459	1.5000	1.1807	1.8600	1.0889
3.3600	2.5613	1.8900	1.3978	2.4600	1.3238
4.0200	2.8377	2.2800	1.5925	3.0300	1.5446
4.7400	3.0953	2.7000	1.7837	3.5850	1.7244
5.5050	3.3384	3.2400	1.9919	4.1400	1.8978
6.3000	3.5665	3.6600	2.1519	4.7400	2.0660
7.1550	3.7849	4.1550	2.3231	5.4720	2.2603
8.0100	3.9807	4.6800	2.4931	6.2700	2.4558
8.9700	4.1814	5.2650	2.6737	7.1520	2.6490
9.9600	4.3810	6.0300	2.8808	8.0400	2.8300
		6.7800	3.0646	8.9700	2.9972
		7.5900	3.2459	9.9150	3.1609
		8.3700	3.4153		
		9.2100	3.5751		
		10.0050	3.7132		

1 MPa. The adsorption equilibrium data of the $CH_4 + N_2 + H_2$ mixture with different compositions were collected for the same temperatures but for lower pressures of up to 6×10^5 Pa. The experimental conditions in different runs are given in Table 4, and the experimental data obtained are listed in Tables 5−11, where p is not the total pressure but the sum of the partial pressures of components and n_t is the sum of the component adsorbed amounts.

Model Description

Most models for predicting the multicomponent adsorption equilibrium are based on the model of single component adsorption equilibrium. Model parameters evaluated from the single component adsorption were then used in the model for predicting the equilibrium of multicomponent adsorption.

Description of the Single Component Adsorption Models. The adsorption equilibrium of pure gases was measured for each component, and then, the data were fitted to an isotherm model. The parameters contained in a model were evaluated in the process of data fitting.

The Langmuir Equation. The well-known Langmuir model fits typical type I isotherms. It is usually expressed in the form of fractional surface coverage:

$$\theta = \frac{n}{n^0} = \frac{bp}{1 + bp} \tag{3}$$

There are two parameters in the model: the saturation adsorption capacity, n^0, and the affinity coefficient, b, which are to be evaluated for each component.

Table 2. Adsorption Data of N_2 on Activated Carbon JX101

T/K					
283		298		313	
$10^{-5}p$/Pa	n/mmol·g^{-1}	$10^{-5}p$/Pa	n/mmol·g^{-1}	$10^{-5}p$/Pa	n/mmol·g^{-1}
.1950	.0863	.1800	.0400	.2250	.0489
.4800	.1965	.3900	.0942	.5100	.1152
.9000	.3472	.5700	.1566	.8400	.1895
1.3650	.4988	.8400	.2278	1.2600	.2731
1.8000	.6341	1.0950	.2964	1.6950	.3638
2.2500	.7608	1.4700	.3880	2.1750	.4491
2.7300	.8790	1.8450	.4729	2.7450	.5437
3.2400	1.0068	2.1900	.5437	3.3300	.6388
3.7800	1.1261	2.5200	.6141	3.9600	.7351
4.3680	1.2522	2.8800	.6897	4.6800	.8408
5.0700	1.3928	3.2700	.7661	5.4600	.9482
5.8200	1.5360	3.6900	.8565	6.2700	1.0520
6.6000	1.6708	4.3500	.9705	7.0800	1.1513
7.4100	1.7995	4.9650	1.0790	7.8900	1.2485
8.2500	1.9219	5.5650	1.1760	8.7000	1.3523
9.2250	2.0557	6.1350	1.2655	9.6300	1.4462
10.2300	2.1900	6.6900	1.3457	10.3650	1.5211
		7.3500	1.4329		
		8.0400	1.5298		
		8.9550	1.6365		
		9.8100	1.7350		

Table 3. Adsorption Data of H_2 on Activated Carbon JX101

T/K					
283		298		313	
$10^{-5}p$/Pa	n/mmol·g^{-1}	$10^{-5}p$/Pa	n/mmol·g^{-1}	$10^{-5}p$/Pa	n/mmol·g^{-1}
.3900	.0116	.6300	.0171	.7100	.0146
.8400	.0287	.9300	.0287	1.3950	.0338
1.2750	.0500	1.2000	.0396	2.0800	.0519
1.7100	.0668	1.6200	.0495	2.7500	.0722
2.1600	.0883	2.0400	.0638	3.4350	.0889
2.6400	.1059	2.5200	.0818	4.0850	.1046
3.2250	.1277	2.9400	.0918	4.9400	.1303
3.9600	.1565	3.4800	.1089	5.8450	.1554
4.7100	.1834	3.9600	.1247	6.7850	.1816
5.4750	.2150	4.5300	.1425	7.7150	.2063
6.2700	.2448	5.1000	.1648	8.5650	.2307
7.0050	.2669	5.7300	.1841	9.4450	.2510
7.8750	.2981	6.4800	.2105	10.3200	.2732
8.7600	.3295	7.2000	.2318		
9.7950	.3657	7.9800	.2567		
		8.7300	.2765		
		9.4650	.2981		
		10.2000	.3219		

Table 4. Experimental Conditions of Multicomponent Adsorption

run	T/K	$100y_{CH_4}$	$100y_{N_2}$	$100y_{H_2}$
1a	283	36.48	27.75	35.77
1b	298	36.48	27.75	35.77
1c	313	36.48	27.75	35.77
2	298	52.78	23.61	23.61
3	298	25.27	23.80	50.93
4	298	30.188	44.925	24.887
5	298	28.47	12.03	59.50

Table 5. Equilibrium Data Obtained in Run 1a

	amount adsorbed/mmol·g^{-1}			
p/100 kPa	n_{CH_4}	n_{N_2}	n_{H_2}	n_t
0.5671	0.3707	7.695×10^{-2}	1.108×10^{-2}	0.4587
1.051	0.5921	0.1130	1.856×10^{-2}	0.7237
1.555	0.7779	0.1436	2.76×10^{-2}	0.9491
2.109	0.9422	0.1742	3.69×10^{-2}	1.153
2.607	1.1041	0.2056	4.325×10^{-2}	1.353
3.167	1.2476	0.2397	5.379×10^{-2}	1.541
3.908	1.4375	0.2800	6.686×10^{-2}	1.784
4.761	1.6277	0.3163	8.284×10^{-2}	2.027
5.779	1.8463	0.3638	9.935×10^{-2}	2.310

Table 6. Equilibrium Data Obtained in Run 1b

	amount adsorbed/mmol·g^{-1}			
p/100 kPa	n_{CH_4}	n_{N_2}	n_{H_2}	n_t
0.5773	0.2639	5.592×10^{-2}	8.580×10^{-3}	0.3284
1.105	0.4401	8.753×10^{-2}	1.556×10^{-2}	0.5432
1.554	0.5824	0.1133	2.253×10^{-2}	0.7182
2.123	0.7159	0.1402	3.061×10^{-2}	0.8868
2.610	0.8340	0.1677	3.774×10^{-2}	1.0395
3.183	0.9657	0.1966	4.674×10^{-2}	1.209
3.954	1.127	0.2290	5.467×10^{-2}	1.411
4.771	1.279	0.2589	6.652×10^{-2}	1.605
5.763	1.451	0.2989	8.126×10^{-2}	1.832

Table 7. Equilibrium Data Obtained in Run 1c

	amount adsorbed/mmol·g^{-1}			
p/100 kPa	n_{CH_4}	n_{N_2}	n_{H_2}	n_t
0.6015	0.1917	4.541×10^{-2}	7.98×10^{-3}	0.2451
1.068	0.3055	6.877×10^{-2}	1.056×10^{-2}	0.3849
1.533	0.4179	9.089×10^{-2}	1.793×10^{-2}	0.5268
2.133	0.5303	0.1174	2.481×10^{-2}	0.6725
2.586	0.6149	0.1321	3.035×10^{-2}	0.7774
3.170	0.7248	0.1574	3.596×10^{-2}	0.9181
3.951	0.8528	0.1868	4.789×10^{-2}	1.088
4.799	0.9944	0.2123	5.859×10^{-2}	1.265
5.778	1.108	0.2420	7.003×10^{-2}	1.420

Table 8. Equilibrium Data Obtained in Run 2

	amount adsorbed/mmol·g^{-1}			
p/100 kPa	n_{CH_4}	n_{N_2}	n_{H_2}	n_t
0.6411	0.3982	4.93×10^{-2}	7.42×10^{-3}	0.4549
1.035	0.5772	6.958×10^{-2}	1.19×10^{-2}	0.6587
1.574	0.7876	8.718×10^{-2}	1.682×10^{-2}	0.8916
2.065	0.9562	0.1096	2.215×10^{-2}	1.088
2.531	1.1105	0.1324	2.546×10^{-2}	1.268
3.077	1.276	0.1566	3.553×10^{-2}	1.468
3.779	1.472	0.1869	4.01×10^{-2}	1.699
4.635	1.687	0.2130	5.041×10^{-2}	1.950
5.660	1.895	0.2439	6.338×10^{-2}	2.202

Table 9. Equilibrium Data Obtained in Run 3

	amount adsorbed/mmol·g^{-1}			
p/100 kPa	n_{CH_4}	n_{N_2}	n_{H_2}	n_t
0.6469	0.2108	5.916×10^{-2}	1.658×10^{-2}	0.2866
1.024	0.3054	7.639×10^{-2}	2.777×10^{-2}	0.4096
1.547	0.4185	0.1014	3.978×10^{-2}	0.5598
2.113	0.5301	0.1277	5.038×10^{-2}	0.7082
2.541	0.6181	0.1514	5.953×10^{-2}	0.8289
3.255	0.7453	0.1825	7.778×10^{-2}	1.006
4.016	0.8580	0.2165	9.971×10^{-2}	1.174
4.862	0.9895	0.2460	0.1170	1.352
5.836	1.122	0.2816	0.1401	1.544

The Langmuir−Freundlich (L−F) Equation. There is one more parameter compared to the Langmuir equation to account for the surface heterogeneity:

$$\theta = \frac{n}{n^0} = \frac{(bp)^q}{1 + (bp)^q} \tag{4}$$

The parameter q is considered as an index of the surface heterogeneity.

Table 10. Equilibrium Data Obtained in Run 4

	amount adsorbed/mmol·g^{-1}			
p/100 kPa	n_{CH_4}	n_{N_2}	n_{H_2}	n_t
0.6502	0.2419	0.1073	7.45×10^{-3}	0.3566
1.023	0.3512	0.1500	1.214×10^{-2}	0.5133
1.515	0.4778	0.1898	1.786×10^{-2}	0.6854
2.078	0.6022	0.2228	2.419×10^{-2}	0.8491
2.566	0.7053	0.2668	3.104×10^{-2}	1.0032
3.205	0.8342	0.3272	4.179×10^{-2}	1.203
3.9859	0.9691	0.3723	5.055×10^{-2}	1.392
4.827	1.108	0.4157	5.926×10^{-2}	1.583
5.845	1.257	0.5061	7.142×10^{-2}	1.835

Table 11. Equilibrium Data Obtained in Run 5

	amount adsorbed/mmol·g^{-1}			
p/100 kPa	n_{CH_4}	n_{N_2}	n_{H_2}	n_t
0.6491	0.2374	2.962×10^{-2}	1.694×10^{-2}	0.2839
1.020	0.3440	4.117×10^{-2}	2.718×10^{-2}	0.4123
1.531	0.4634	4.862×10^{-2}	4.295×10^{-2}	0.5549
2.085	0.5912	6.286×10^{-2}	5.563×10^{-2}	0.7097
2.580	0.6929	7.635×10^{-2}	7.11×10^{-2}	0.8403
3.215	0.8180	8.908×10^{-2}	8.445×10^{-2}	0.9916
3.941	0.9388	0.1047	0.1032	1.147
4.826	1.090	0.1243	0.1262	1.340
5.822	1.244	0.1413	0.1553	1.541

The Flory−Huggins Vacancy Solution Model (FHVSM). The vacancy solution model in conjunction with the Flory−Huggins activity coefficient equation yields an adsorption isotherm equation for a single component:

$$p = \left(\frac{n^0}{b}\frac{\theta}{1-\theta}\right)\exp\left(\frac{{a_{1v}}^2\theta}{1 + a_{1v}\theta}\right) \tag{5}$$

As in the L−F model, there are three parameters to be evaluated in data fitting: n^0, b, and a_{1v}.

The MPSD−Langmuir Model. The MPSD model assumes that the surface heterogeneity of the adsorbent is induced solely by the micropore size distribution (MPSD). Assuming a distribution function, $f(r)$, for MPSD, one can have the amount adsorbed of a single component, i, as the integral of the local isotherm, $n_i(r, P, T)$, over an appropriate range of micropore sizes for the component. That is,

$$n_i = \int_{r_1}^{r_2} n_i(r, P, T)\, f(r)\, \mathrm{d}r \tag{6}$$

where r_1 and r_2 are the lower and upper limits of the pore half-width accessible to the adsorbate, respectively. The local adsorption isotherm assumes the following form of the Langmuir equation:

$$n_i(r, P, T) = {n_i}^0(T)\frac{b(r)P}{1 + b(r)P} \tag{7}$$

The parameter b is defined as the local affinity, which is a function of pore size, r, and temperature:

$$b(r) = b_\infty \exp\left[\frac{E(r)}{RT}\right] \tag{8}$$

where b_∞ is the adsorption affinity at temperature infinity and $E(r)$ is the adsorbate−pore interaction energy, which is taken as the negative of the adsorption potential minimum and is a function of pore size. For slit-shaped micropores, as was assumed for activated carbon, the potential energy was usually calculated with the 10-4-3

form of the Lennard-Jones equation. Gamma distribution was assumed for the MPSD:

$$f(r) = \frac{q^{v+1} r^{v} \exp(-qr)}{\Gamma(1+v)} \tag{9}$$

where q and v are the distribution parameters. Finally, the adsorption isotherm for a single component, i, was expressed explicitly as

$$n_i = \int_{r_{\min,i}}^{\infty} n_i^{0} \frac{b_{0,i} \exp[E(r,i)/RT] p_i}{1 + b_{0,i} \exp[E(r,i)/RT] p_i} \frac{q^{v+1} r^{v} \exp(-qr)}{\Gamma(1+v)} \, \mathrm{d}r \tag{10}$$

where $r_{\min,i}$ is the minimum half-width accessible to the adsorbate molecules. Pore size distribution is regarded as an intrinsic characteristic of the adsorbent; therefore, the parameters characterizing carbon structure (q and v) and the isotherm parameters (n_i^0 and $b_{0,i}$) were determined on the basis of simultaneous optimization in fitting the model to the isotherm data of different adsorbates at multiple temperatures.

Description of the Multicomponent Adsorption Models. *The Extended Langmuir (EL) Model*. In extending the Langmuir equation into the multicomponent system, all assumptions made for the adsorption of pure gases are maintained. The amount adsorbed of component i becomes

$$\theta_i = \frac{n_i}{n_i^{0}} = \frac{b_i p_i}{1 + \sum_{i=1}^{m} b_i p_i} \tag{11}$$

The extended Langmuir equation might be the simplest model for multicomponent adsorption. It is expressed analytically and explicitly; therefore, it yields a much faster computation for the study of adsorption dynamics. However, this model is inadequate for representing a real adsorption system. Sometimes the Langmuir equation cannot fully describe the adsorption data of single components either. In addition, the thermodynamic consistency requires that the saturation adsorption capacity is the same for all components,[25] but such assumption is unrealistic for molecules of widely different sizes. The parameter values of the saturation adsorption capacity obtained from the model of single component adsorption differ from species to species. The prediction accuracy must be affected if this parameter takes one value for all the components.

The Loading Ratio Correlation (LRC) Model. The Langmuir−Freundlich equation was extended to multicomponent adsorption in the same way as was done for the Langmuir equation:

$$\theta_i = \frac{n_i}{n_i^{0}} = \frac{(b_i p_i)^{q_i}}{1 + \sum_{i=1}^{m} (b_i p_i)^{q_i}} \tag{12}$$

The extended equation was usually named as the loading ratio correction (LRC) model. It allows for the effect of surface energetic heterogeneity. Because of its mathematical simplicity, the LRC model is frequently applied in dynamics studies of adsorption columns. However, this model does not have a sound theoretical foundation, which should be kept in mind in application. Besides, it has the same problem with the parameter of saturation adsorption capacity as was encountered in the extended Langmuir equation.

The Ideal Adsorption Solution Theory (IAST). Myers and Prausnitz proposed an IAST based on a sound thermodynamic framework.[6] If the adsorbed phase is thermodynamically ideal, the equilibrium relationships for the adsorption of a mixture can be derived directly from the isotherms of pure components. Integration of a pure component isotherm according to the Gibbs equation yields the relationship between the spreading pressure and the equilibrium pressure for each component:

$$\frac{\pi_i^{0} A}{RT} = \int_0^{p_i^{0}} \frac{n_i}{p} \, \mathrm{d}p \tag{13}$$

The Langmuir equation was usually used to describe the adsorption isotherm of single components for simplicity. According to the theory of ideal solution,

$$P y_i = P_i^{0}(\pi) x_i \tag{14}$$

It yields for mixing at constant temperature and spreading pressure that

$$\pi_i^{0} = \pi_{\text{mixture}} \tag{15}$$

Specifying two independent variables, p and y_i, the other variables can be calculated. This model has some attractive features. First, the IAST does not require any data of the mixture; second, it is independent of the adsorption model of pure gases, since it is an application of the solution thermodynamics for the adsorption system.[26] However, the assumption included in the IAST was of limited applicability, and the theory cannot predict nonideal behavior such as the adsorption azeotrope.

The Flory−Huggins Vacancy Solution Model (FHVSM). The FHVSM treated the adsorption equilibrium as an osmotic equilibrium between two "vacancy" solutions having different compositions. Vacancy is an imaginary entity defined as a vacuum space that acts as the solvent of the system. The nonideality of the adsorbed solution is accounted for in terms of the activity coefficient. The dependence of the coefficient on composition is described by the Flory−Huggins equation. This model accounts for the adsorbate−adsorbate interaction based only on the pure gas data. For multicomponent adsorption equilibrium, the distribution of the adsorbate between the gas and the adsorbed phase can be obtained by equating the chemical potentials of the adsorbate in two phases:

$$\phi_i p y_i = \gamma_i^{s} x_i \frac{n_t}{n_t^{0}} \frac{n_i^{0}}{b_i} \left[\frac{\exp(a_{iv})}{1 + a_{iv}}\right] \exp\left\{\left[\frac{n_i^{0} - n_t^{0}}{n_t} - 1\right] \ln \gamma_v^{s} x_v^{s}\right\} \tag{16}$$

where γ_i^s is the Flory−Huggins activity coefficient, which is given by

$$\ln \gamma_i^{s} = -\ln \sum_{j=1}^{j=4} \frac{x_j^{s}}{a_{ij}} + 1 + \left[1 - \left(\sum_{j=1}^{j=4} \frac{x_j^{s}}{a_{ij}} + 1\right)^{-1}\right] \tag{17}$$

Solution was obtained by a trial-and-error method.

The Micropore Size Distribution−Extended Langmuir (MPSD−EL) Model. Equation 10 was extended to the

Table 12. Langmuir Parameters for the Adsorption of Pure CH_4, N_2, and H_2 on Activated Carbon JX101

component	T/K	$10^{-5}b$/Pa^{-1}	n^0/mmol·g^{-1}	ARD/%
methane	283	0.2073	6.367	4.20
	298	0.1541	6.041	2.68
	313	0.1215	5.724	1.45
nitrogen	283	0.0847	4.677	2.07
	298	0.0610	4.637	2.38
	313	0.0522	4.307	1.47
hydrogen	283	0.00973	4.206	4.65
	298	0.00123	26.0914	2.70
	313	5.7266×10^{-6}	4.6362×10^3	4.36

multicomponent system in the same way that the Langmuir equation was extended:

$$n_i = \int_{r_{\min,i}}^{\infty} n_i^0 \frac{b_{0,i} \exp(E(r,i)/RT) p_i}{1 + \sum_{j=1}^{m} b_{0,j} \exp(E(r,j)/RT) p_j} \frac{q^{v+1} r^v \exp(-qr)}{\Gamma(1+v)} \mathrm{d}r \quad (18)$$

The parameters contained were optimized on the basis of the data of single component adsorption.

The Micropore Size Distribution−Ideal Adsorption Solution Theory (MPSD−IAST) Model. The MPSD−EL model has an explicit local isotherm; therefore, it is quite convenient for simulation computations. However, the equal saturation capacity constraint for different components will seriously affect the fitness of the model to the equilibrium data of pure component adsorption and, hence, results in a poor prediction of the multicomponent adsorption equilibrium. The ideal adsorbed solution theory (IAST) offers an alternative solution. The MPSD−IAST model assumes that micropore size distribution (MPSD) represents the energetic heterogeneity of the adsorbent and uses the ideal adsorbed solution theory to describe the local multicomponent adsorption equilibrium within a given pore.

Applicability Test on the Models with Experimental Data

The fitness of different models to the experimental data is expressed as the average relative discrepancy (ARD), which is defined as the average of the relative difference between the experimental data and that predicted by a model:

$$\mathrm{ARD} = \frac{1}{N} \sum_{i=1}^{N} \left| \frac{v_{i,\mathrm{exptl}} - v_{i,\mathrm{calcd}}}{v_{i,\mathrm{exptl}}} \right| \times 100 \quad (19)$$

where $v_{i,\mathrm{exptl}}$ is the ith experimental value of a variable and $v_{i,\mathrm{calcd}}$ is the corresponding value calculated with a model and N is the total number of points in a data set. The arithmetic mean of ARD(v)'s over all components is called the general average relative discrepancy of a model (GARD(v)):

$$\mathrm{GARD}(v) = \frac{1}{M} \sum_{i=1}^{M} v_i \quad (20)$$

where M is the number of components in the mixture.

Verification of the Single Component Adsorption Models. Models for the single component adsorption were fitted to the experimental isotherms of pure CH_4, N_2, and H_2 by nonlinear regression, respectively. The evaluated parameters are listed in Tables 12−15 for each component.

Table 13. L−F Parameters for the Adsorption of Pure CH_4, N_2, and H_2 on Activated Carbon JX101

component	T/K	$10^{-5}b$/Pa^{-1}	n^0/mmol·g^{-1}	q	ARD/%
methane	283	0.1097	8.4168	0.8233	1.52
	298	0.1125	7.0125	0.91229	4.03
	313	0.0907	6.6222	0.9288	1.93
nitrogen	283	0.0580	5.7337	0.9262	0.52
	298	0.06317	4.5435	1.0064	2.32
	313	0.0329	5.6808	0.9357	1.72
hydrogen	283	0.02494	1.9963	1.0648	3.06
	298	0.01698	2.44883	1.07739	1.88
	313	0.02182	1.74853	1.12929	1.31

Table 14. FHVSM Parameters for the Adsorption of Pure CH_4, N_2, and H_2 on Activated Carbon JX101

component	T/K	$10^{-5}b$/ mmol·g^{-1}·Pa	n^0/mmol·g^{-1}	a_{1v}	ARD/%
methane	283	1.8848	8.8395	1.6938	0.77
	298	1.1271	8.0250	1.3010	3.40
	313	0.7908	7.6945	1.1707	1.51
nitrogen	283	0.4311	6.7217	1.1353	0.59
	298	0.3025	8.0181	1.3050	3.57
	313	0.2394	17.8291	2.3715	0.90
hydrogen	283	0.04097	4.1548	0.1114	4.67
	298	0.03217	9.70745	0.00023	3.01
	313	0.026816	22	-8.0272×10^{-8}	4.73

Table 15. MPSD Parameters for the Adsorption of Pure CH_4, N_2, and H_2 on Activated Carbon JX101

component	T/K	n^0/ mmol·g^{-1}	$10^{-5}b$/Pa^{-1}	q	v	ARD/%
methane	283	10.0222	4.3139×10^{-5}	21.5400	91.1036	0.75
	298	9.9419	4.4436×10^{-5}	21.5400	91.1036	2.71
	313	9.5713	4.9519×10^{-5}	21.5400	91.1036	1.16
nitrogen	283	7.1849	1.9706×10^{-4}	21.5400	91.1036	0.74
	298	7.4392	1.7863×10^{-4}	21.5400	91.1036	2.83
	313	6.6486	2.0915×10^{-4}	21.5400	91.1036	1.03
hydrogen	283	5.1454	7.0694×10^{-4}	21.5400	91.1036	4.59
	298	12.365	2.6624×10^{-4}	21.5400	91.1036	2.93
	313	18.243	1.6687×10^{-4}	21.5400	91.1036	4.86

Table 16. Performance of the EL Model for the Adsorption of a $CH_4 + N_2 + H_2$ Mixture on Activated Carbon JX101

run	$100\Delta n_{CH_4}$	$100\Delta n_{N_2}$	$100\Delta n_{H_2}$	100GARD(n)	100GARD(x)
1a	13.0	10.4	34.4	19.3	14.4
1b	13.4	6.7	33.1	17.8	12.6
1c	9.8	8.1	30.0	16.0	11.8
2	12.0	4.84	44.7	20.5	16.3
3	16.0	7.27	42.4	21.9	15.3
4	16.0	8.53	44.8	23.1	16.3
5	14.7	8.53	37.4	20.2	13.8

The fitness of a model expressed by the average relative discrepancy (ARD) is shown in the last column of each table. The relative discrepancy of these models is <5% for the range tested. Therefore, these isotherm models fit the adsorption equilibrium data of single components quite well.

Verification of the Multicomponent Adsorption Models. On the basis of the adsorption isotherms of pure components and the model parameters evaluated thereof, one can calculate the amount adsorbed of each component in a mixture using the models described previously. The average relative discrepancy of a model in predicting the component adsorption, Δn_i, was calculated by eq 19 for each condition tested and is listed in Tables 16−21. The composition of the adsorbed phase can be determined on the basis of the values of n_i, and the ARDs for the molar fraction of components could also be determined. The general average relative discrepancies of a model in predicting adsorption and composition (GARD(n) and

Table 17. Performance of the LRC Model for the Adsorption of a $CH_4 + N_2 + H_2$ Mixture on Activated Carbon JX101

run	$100\Delta n_{CH_4}$	$100\Delta n_{N_2}$	$100\Delta n_{H_2}$	100GARD(n)	100GARD(x)
1a	4.1	16.7	35. 8	18.9	18.1
1b	9.5	7.6	37.5	18.2	14.2
1c	5.8	9.8	39.9	18.5	17.1
2	9.6	6.5	49.4	21.8	18.4
3	10.4	7.7	45.2	21.1	16.7
4	10.9	9.3	50.1	23.4	19.1
5	10.0	8.2	39.8	19.3	15.5

Table 18. Performance of the IAST for the Adsorption of a $CH_4 + N_2 + H_2$ Mixture on Activated Carbon JX101

run	$100\Delta n_{CH_4}$	$100\Delta n_{N_2}$	$100\Delta n_{H_2}$	100GARD(n)	100GARD(x)
1a	12.1	7.2	37.5	18.9	14.1
1b	13.1	4.8	28.2	15.4	9.9
1c	9.5	6.6	24.6	13.6	9.3
2	11.8	5.9	39.6	19.1	13.3
3	15.8	6.5	39.2	20.5	13.4
4	15.4	7.7	40.8	21.3	13.8
5	14.8	6.9	34.1	18.6	11.8

Table 19. Performance of the FHVSM for the Adsorption of a $CH_4 + N_2 + H_2$ Mixture on Activated Carbon JX101

run	$100\Delta n_{CH_4}$	$100\Delta n_{N_2}$	$100\Delta n_{H_2}$	100GARD(n)	100GARD(x)
1a	2.7	5.5	24.9	11	8.3
1b	7.3	6.3	26.2	13.3	7.5
1c	3.8	8.0	22.7	11.5	9.6
2	7.6	8.6	37.7	18	12.1
3	8.4	7.4	37.8	17.9	12.5
4	9.1	8. 1	38. 9	18.7	12.4
5	7.5	6.6	32.8	15.6	11.1

Table 20. Performance of the MPSD−EL Model for the Adsorption of a $CH_4 + N_2 + H_2$ Mixture on Activated Carbon JX101

run	$100\Delta n_{CH_4}$	$100\Delta n_{N_2}$	$100\Delta n_{H_2}$	100GARD(n)	100GARD(x)
1a	6. 6	7.4	32.2	15.4	12.1
1b	9.0	4.9	29.8	14.6	10.0
1c	6.5	7.3	26.9	13.6	10.2
2	8.8	4.9	41.2	18.3	13.9
3	10. 5	6.0	40. 3	18.9	14.1
4	11.2	7.3	42. 1	19.7	14.5
5	9.3	6.8	35. 2	17.1	12.6

Table 21. Performance of the MPSD−IAST Model for the Adsorption of a $CH_4 + N_2 + H_2$ Mixture on Activated Carbon JX101

run	$100\Delta n_{CH_4}$	$100\Delta n_{N_2}$	$100\Delta n_{H_2}$	100GARD(n)	100GARD(x)
1a	5.3	4.7	37.2	15.7	12.4
1b	8.4	5.5	28.8	14.2	8.6
1c	5.9	5.2	24.9	12.0	8.4
2	8.3	7.5	40.2	18.7	12.8
3	9.9	7.0	39.6	18.9	13.2
4	10.2	7.8	41.1	20.2	13.2
5	9.1	6.2	34.6	16.6	11.7

GARD(x)) were calculated with eq 20 and listed in the last two columns of these tables. To make a clear comparison, these data are put together in Figures 4 and 5. As is seen from the tables, the ARDs of most models for CH_4 and N_2 are reasonable, but no one model yields a reasonable ARD for H_2. Hydrogen is a weakly adsorbed species, and a small experimental error will cause a great relative discrepancy;[14] therefore, the weakly adsorbed component, hydrogen, cannot be well predicted. The value of GARD(x) is remarkably less than GARD(n) because the content of H_2 in the adsorbed phase is much less than CH_4 and N_2. Although not rigorous, GARD is a reasonable representative index of model performance.

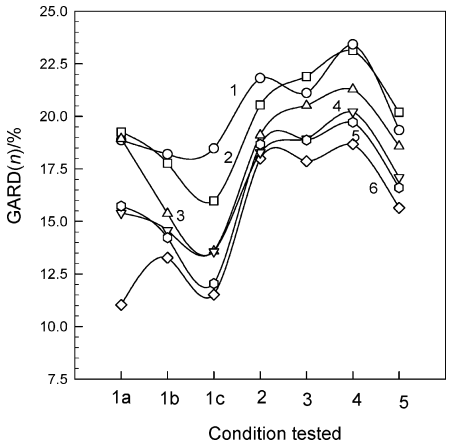

Figure 4. General average relative discrepancy of models in predicting the amounts adsorbed from the mixture $CH_4 + N_2 + H_2$ onto activated carbon: 1, LRC; 2, EL; 3, IAST; 4, MPSD−EL; 5, MPSD−IAST; 6, FHVSM.

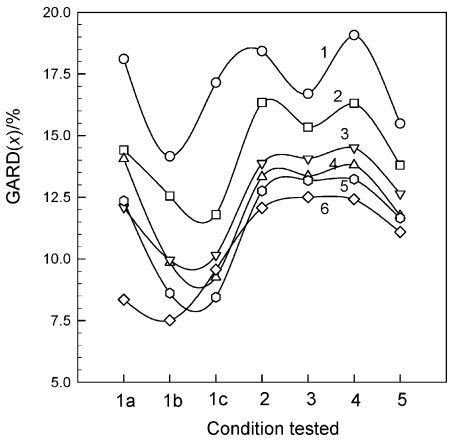

Figure 5. General average relative discrepancy of models in predicting the composition of the adsorbed phase for the mixture $CH_4 + N_2 + H_2$ on activated carbon: 1, LRC; 2, EL; 3, MPSD−EL; 4, IAST; 5, MPSD−IAST; 6, FHVSM.

Discussion and Conclusions

Some models for predicting multicomponent adsorption are based on a model of single component adsorption; therefore, the fitness of the single component adsorption model to the experimental data is a prerequisite yet not a complete condition that guarantees the fitness of the multicomponent adsorption model. For example, The Langmuir−Freundlich model is good for single component adsorption; however, the LRC model, obtained by extending the L−F model to the multicomponent system, is worse than the others, as shown in Figures 4 and 5.

Most models tested work well for the components CH_4 and N_2, but no one model is good for the component H_2 and, hence, for mixtures containing H_2. This might be caused by the large difference in the adsorption affinity between components.

The average relative discrepancy of models in predicting the composition of the adsorbed phase is ~5% less than that in predicting the amount adsorbed. The sequence of model performance is a little different too.

The FHVSM seems superior over the others in predicting the adsorption equilibrium of the testing mixture; however, the ARD for H_2 is also as high as 25% to 40%. Nonetheless, the GARDs in predicting both composition and the amount adsorbed are the lowest. The models based on micropore size distribution and the IAST also work well. The EL and

LRC models are the most convenient to use but show the largest discrepancy with the experimental data, although the difference with other models is not very much.

Literature Cited

(1) Wang, K.; Do, D. D. Single and Multicomponent Adsorption Equilibria of Hydrocarbons on Activated Carbon: The Role of Micropore Size Distribution. *Surfactant Sci. Ser*. **1999**, *78*, 391−441.

(2) Hu, X.; Do, D. D. Multicomponent Adsorption Kinetics of Hydrocarbons onto Activated Carbon: Effect of Adsorption Equilibrium Equations. *Chem. Eng. Sci*. **1992**, *47*, 1715−1725.

(3) Ruthven, D. M. *Principles of Adsorption and Adsorption Processes*; Wiley: New York, 1984.

(4) Yang, R. T. *Gas Separation by Adsorption Processes*; Butterworth: Boston, MA, 1987.

(5) Do, D. D. *Adsorption Analysis: Equilibria & Kinetics*; Imperial College: London, 1998.

(6) Myers, A. L.; Prausnitz, J. M. Thermodynamics of Mixed-Gas Adsorption. *AIChE J*. **1965**, *11*, 121−127.

(7) Suwanayuen, S.; Danner, R. P. A Gas Adsorption Isotherm Equation Based on Vacancy Solution Theory. *AIChE J*. **1980**, *26*, 68−75.

(8) Suwanayuen, S.; Danner, R. P. Vacancy Solution theory of adsorption from gas mixtures. *AIChE J*. **1980**, *26*, 76−83.

(9) Cochran, T. W.; Knaebel, R. L.; Danner, R. P. Vacancy Solution Theory of Adsorption Using Flory-Huggins Activity Coefficient Equations. *AIChE J*. **1985**, *31*, 268−277.

(10) Hu, X.; Do, D. D. In *Effect of Pore Size Distribution on the Prediction of Multicomponent Adsorption Equilibria. Fundam. Adsorption*; Levan, M. D., Ed.; Kluwer Academic: Boston, MA, 1996; pp 385−392.

(11) Wang, K.; Do, D. D. Characterizing the Micropore Size Distribution of Activated Carbon Using Equilibrium Data of Many Adsorbates at Various Temperatures. *Langmuir* **1997**, *13*, 6226−6233.

(12) Hu, X. Multicomponent Adsorption Equilibrium of Gases in Zeolite: Effect of Pore Size Distribution. *Chem. Eng. Commun*. **1999**, *174*, 201−214.

(13) Qiao, S.; Wang, K.; Hu, X. Study of Binary Adsorption Equilibrium of Hydrocarbons in Activated Carbon Using Micropore Size Distribution. *Langmuir* **2000**, *16*, 5130−5136.

(14) Qiao, S.; Wang, K.; Hu, X. Using Local IAST with Micropore Size Distribution to Predict Multicomponent Adsorption Equilibrium of Gases in Activated Carbon. *Langmuir* **2000**, *16*, 1292−1298.

(15) Wang, K.; Qiao, S.; Hu, X. Application of IAST in the Prediction of Multicomponent Adsorption Equilibrium of Gases in Heterogeneous Solids: Micropore Size Distribution versus Energy Distribution. *Ind. Eng. Chem. Res*. **2000**, *39*, 527−532.

(16) Zhou, Y.-P.; Zhou, L. Experimental Study on High-Pressure Adsorption of Hydrogen on Activated Carbon. *Sci. China, Ser. B* **1996**, *39*, 598−607.

(17) Zhou, L.; Bai, S.-P.; Su, W.; Yang, J.; Zhou, Y.-P. Comparative Study of the Excess versus Absolute Adsorption of CO_2 on Superactivated Carbon for the Near-Critical Region, *Langmuir* **2003**, *19*, 2683−2690.

(18) Dreisbach, F.; Staudt, R.; Keller, J. U. High Pressure Adsorption Data of Methane, Nitrogen, Carbon Dioxide and their Binary and Ternary Mixtures on Activated Carbon. *Adsorption* **1999**, *5*, 215−227.

(19) Keller, J. U.; Dreisbach, F.; Rave, H.; Staudt, R.; Tomalla, M. Measurements of Gas Mixture Adsorption Equilibria of Natural Gas Compounds on Microporous Sorbents. *Adsorption* **1999**, *5*, 199−214.

(20) Mayfield, P. L. J.; Do, D. D. Measurement of the Single-Component Adsorption Kinetics of Ethane, Butane, and Pentane onto Activated Carbon Using a Differential Adsorption Bed. *Ind. Eng. Chem. Res*. **1991**, *30*, 1262−1270.

(21) Siddiqi, K. S.; Thomas, W. J. The adsorption of methane-ethane mixtures on activated carbon. *Carbon* **1982**, *20*, 473−479.

(22) Wu, Q. Studies on Multicomponent Adsorption Equilibrium of Supercritical Gas Mixture on Porous Solids. Doctor Thesis, School of Chemical Engineering and Technology, Tianjin University, Tianjin, China, 2003.

(23) Malek, A.; Farooq, S. Effect of Velocity Variation due to Adsorption-Desorption on Equilibrium Data from Breakthrough Experiments. *Chem. Eng. Sci*. **1995**, *50*, 737−740.

(24) Malek, A.; Farooq, S. Determination of Equilibrium Isotherms Using Dynamic Column Breakthrough and Constant Flow Equilibrium Desorption. *J. Chem. Eng. Data* **1996**, *41*, 25−32.

(25) Hu, X.; Do, D. D. Comparing Various Multicomponent Adsorption Equilibrium Models. *AIChE J*. **1995**, *41*, 1585−1592.

(26) Ahmadpour, A.; Wang, K.; Do, D. D. Comparison of Models on the Prediction of Binary Equilibrium Data of Activated Carbons. *AIChE J*. **1998**, *44*, 740−752.

Received for review October 9, 2004. Accepted December 6, 2004. The work is supported by the National Natural Science Foundation of China (#20336020).

JE049643A